INSTITUTE OF PHYSICS PUBLISHING SUPERCONDUCTOR SCIENCE AND TECHNOLOGY

Supercond. Sci. Technol. **19** (2006) S60–S66 doi:10.1088/0953-2048/19/3/009

Predicting AC loss in practical superconductors

F Gömöry[1], J Šouc[1], M Vojenčiak[1], E Seiler[1], B Klinčok[1], J M Ceballos[1,2], E Pardo[1,3], A Sanchez[3], C Navau[3], S Farinon[4] and P Fabbricatore[4]

[1] Institute of Electrical Engineering, Slovak Academy of Sciences, Dúbravská cesta 9, 842 39 Bratislava, Slovakia
[2] Department of Electrical Engineering, University of Extremadura, Badajoz, E-06071, Spain
[3] Grup d'Electromagnetisme, Departament de Fisica, Universitat Autonoma Barcelona, 08193 Bellaterra (Barcelona), Catalonia, Spain
[4] Istituto Nazionale di Fisica Nucleare, Via Dodecaneso 33, Genoa, I-16146, Italy

Received 3 October 2005, in final form 21 November 2005
Published 20 January 2006
Online at stacks.iop.org/SUST/19/S60

Abstract

Recent progress in the development of methods used to predict AC loss in superconducting conductors is summarized. It is underlined that the loss is just one of the electromagnetic characteristics controlled by the time evolution of magnetic field and current distribution inside the conductor. Powerful methods for the simulation of magnetic flux penetration, like Brandt's method and the method of minimal magnetic energy variation, allow us to model the interaction of the conductor with an external magnetic field or a transport current, or with both of them. The case of a coincident action of AC field and AC transport current is of prime importance for practical applications. Numerical simulation methods allow us to expand the prediction range from simplified shapes like a (infinitely high) slab or (infinitely thin) strip to more realistic forms like strips with finite rectangular or elliptic cross-section. Another substantial feature of these methods is that the real composite structure containing an array of superconducting filaments can be taken into account. Also, the case of a ferromagnetic matrix can be considered, with the simulations showing a dramatic impact on the local field. In all these circumstances, it is possible to indicate how the AC loss can be reduced by a proper architecture of the composite. On the other hand, the multifilamentary arrangement brings about a presence of coupling currents and coupling loss. Simulation of this phenomenon requires 3D formulation with corresponding growth of the problem complexity and computation time.

(Some figures in this article are in colour only in the electronic version)

1. Introduction

Since the discovery of superconductivity, the disappearance of electrical resistivity motivated many scientists to think about the application of superconductors in electric power engineering. When hard superconductors as materials reaching the demand for competitive current transport capability appeared in the early 1960s, a new problem emerged: it was soon realized that the ability to lead persistent electrical currents is linked with the appearance of dissipation in the AC regime, i.e. at transporting AC current or during exposure to AC magnetic field. This phenomenon, called the AC loss in superconductors, has occupied a significant sector of the superconducting research until now.

In the era of low-temperature superconductors (LTSs), a typical structure of a superconducting wire was established. It contained superconducting filaments in a metallic matrix. The cross-section of such a composite wire had the form of a circle or a rectangle with the aspect ratio of the sides rarely exceeding two, i.e. close to a square. For this metal–superconductor

structure, the fundamental principles of the AC loss mechanism were revealed. It was found that the heat generation can be attributed to electrical currents induced in the composite structure. Several significant paths for current loops have been identified, and two loss dissipation mechanisms distinguished: in the case of screening current forming a loop entirely within the superconducting filament, its creation will cost energy due to the pinning of magnetic flux in the superconductor. This loss component is called the hysteresis loss. Another mechanism is the so-called coupling loss, ascribed to the current flowing in a loop that is mostly formed by superconducting paths, but also contains portions with normal resistance [1–5].

This terminology remains valid in the investigation of wires made from high-temperature superconductors (HTSs). However, several factors have pushed the research of AC loss significantly forward in the recent period. First, the most used HTS wire has the form of a tape, to achieve good alignment of HTS grains. The aspect ratio of the sides of its rectangular cross-section typically exceeds 10. Then, the approximation of an infinite slab in parallel magnetic field, fruitfully applied to the wires and windings from LTS wires, becomes rather doubtful. Also, the composite structure of HTS wires is far less regular than in the case of LTSs. Then, instead of the effective medium approach that successfully explained many of the effects observed in LTS wires, one has to take into consideration the real structure of the composite. On the other hand, tremendous increase of the computing power accessible on a personal computer made available numerical methods that are adequate to cope with the aforementioned complications. It is the main purpose of this paper to encourage non-specialists in numerical simulations to utilize these methods in the investigation of AC applications of superconductors.

In section 2, the properties of simple shapes will be summarized in order to show the general rules that govern the AC loss. The importance of the demagnetizing field to the AC loss will be illustrated. In section 3, the use of two powerful numerical methods allowing us to simulate the behaviour of a superconducting wire in arbitrary conditions will be demonstrated for several cases of practical importance. We will show how the treatment of superconducting material as a conductor with a highly non-linear current–voltage curve allows us to solve the problem of current distribution into parallel paths and to simulate the flux distribution in a cable consisting of a single layer of superconducting tapes. The influence of tape arrangement, in particular the width of gaps between tapes, on the AC loss can be investigated in this way. Also, the method of minimum magnetic energy variation (MMEV) will be presented as a tool to understand the dissipation in the case of simultaneous action of AC field and AC current for a wire with rectangular cross-section. We also show that this method allows us to simulate the critical state and accompanied dissipation in a superconducting wire with ferromagnetic matrix. In section 4 we briefly summarize the presented results.

2. AC loss in hard superconductors with simple shapes

The appearance of dissipation in hard superconductors exposed to a changing magnetic field was recognized simultaneously with the formulation of the critical-state model. This model has served as an excellent approximation of the electromagnetic behaviour of these materials since then [6]. The simplest shape allowing us to derive analytical expressions for the distribution of local magnetic field, current density and electrical field is that of a slab (infinitely high) in a parallel magnetic field. Dissipation in the cyclic regime of external magnetic field $B_{ac} = B_a \sin \omega t$ is easily calculated, showing the following fundamental features.

The dissipation depends on the volume of the sample affected by the movement of flux lines. In the beginning part of the magnetization process, there remains a portion of the sample untouched by the field change because the screening currents, starting from the sample surface, are able to shield the change of applied field completely. This shielding capability is exhausted when the applied field has reached the value called the penetration field B_p. For low fields, i.e. smaller than B_p, the AC loss is proportional to B_a^3. Beyond B_p, the pattern of induced currents is saturated, and the loss increase with B_a is just linear, creating in this way a kink in the AC loss dependence on B_a. The value of penetration field depends on the sample thickness, thus the AC loss is not solely a material property. This was further underlined when samples in perpendicular magnetic field (e.g. single crystals of HTS) started to attract attention. Interestingly, the value of B_p remained roughly the same as that found in parallel field [7], but the losses increased dramatically. Taking into account the enhancement of local magnetic field in perpendicular geometry due to the demagnetizing effect, this observation can be easily explained. The results achieved for AC loss in superconductors of simple shapes exposed to a cyclic AC field can be generally expressed by the following formula [8]:

$$q = S\frac{\pi}{\mu_0}\chi_0 B_a^2 \chi''_{int}(y) \tag{1}$$

where q is the loss per metre length of a superconducting wire, S is its cross-section, $\mu_0 = 4\pi \times 10^{-7}$ H m^{-1}, χ_0 is the initial susceptibility that will be discussed later on and χ''_{int} is the imaginary part of the internal complex magnetic susceptibility. As indicated in the formula, it depends on the variable $y = \frac{B_a}{B_{max}}$, i.e. the AC field amplitude scaled by the value where the susceptibility curve reaches its maximum. For the slab in parallel field $B_{max} \approx B_p$; however, in the perpendicular geometry, e.g. that of a thin strip or disc in a transversal field, the AC susceptibility reaches its maximum well before the complete saturation of the sample cross-section by the critical current density. In theoretical papers dealing with magnetic flux penetration into superconductors of various shapes [6, 9–11], the corresponding $\chi''_{int}(\frac{B_a}{B_{max}})$ curve can be found as well as the value of χ_0. Interestingly, this dependence is rather similar for all the investigated simple shapes, indicating that a significant loss reduction cannot be reached by a simple shape optimization of the conductor [8]. This is illustrated in figure 1. However, the shape factor χ_0 for all the simple shapes can be roughly estimated by the formula

$$\chi_0 = 1 + \frac{a}{b} \tag{2}$$

where a is the wire dimension perpendicular to the applied field and b is the dimension parallel to the applied field. In the

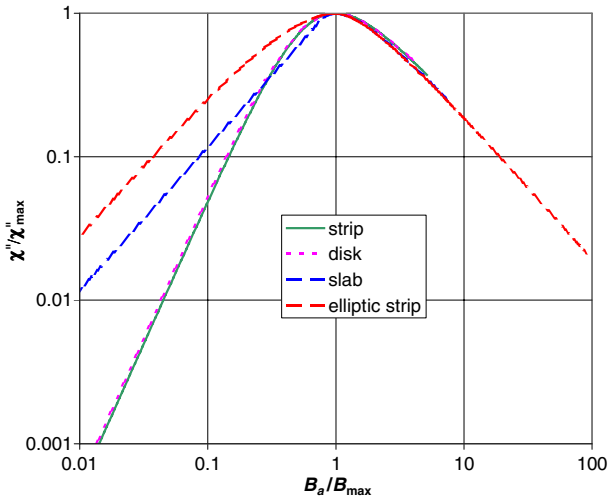

Figure 1. Theoretical prediction of AC loss behaviour—in applied magnetic field—for hard superconductors of various simple shapes. The loss is characterized by the imaginary part of AC susceptibility according to the formula (1). To allow direct comparison of the dependences, the both axes are normalized to make the curves meet at (1, 1).

case of a slab in a parallel field $b \gg a$, thus $\chi_0 \approx 1$. When the field is rotated by 90°, the same slab in a perpendicular field will exhibit $\chi_0 \approx \frac{a}{b} \gg 1$. Thus, the rule of thumb for the magnetization loss reduction is 'avoid perpendicular magnetic field'. This conclusion also remains valid for a rough estimation of magnetization hysteresis loss in an array of filaments [12]. Rigorous analytical derivation of AC loss formulae for an infinite stack or a horizontal array of filaments can be found in [13]. Extensive numerical calculations of AC loss in two-dimensional matrices of filaments have been published [14]. Valuable comparison of AC loss measured on a horizontal array with theoretical predictions obtained by different methods has been published recently [15].

In the case of transporting AC current, the result is even simpler: save very thin strips, with the side aspect ratio exceeding 100, the shape of the superconducting wire does not influence the loss notably [16]. Nevertheless, the distribution of critical current density—or the density of filaments in the case of a multifilamentary wire—would lead to the deviation of this unique behaviour. Generally, the conductor with better properties of the surface filaments will exhibit at low currents a lower AC loss then predicted by the Norris formula [17, 18].

3. Flux penetration into complex shapes

The approximation of superconductors in real windings by one of the models mentioned in the previous paragraph, successfully applied in the LTS era, faces serious problems in the case of HTS wires. The perpendicular geometry was found as the critical arrangement, and the study of tape conductors in perpendicular field became the standard experiment. Fortunately, at the same time the performance of common personal computers increased in a way that allows us to carry out the numerical simulations taking into account the real structure of composite wires.

Systematic investigation for a series of Bi-2223/Ag composites demonstrated the possibility of determining χ_0 with the help of a finite element simulation of the diamagnetic state of superconducting filaments as a linear problem [19]. However, the substantial progress in understanding the loss behaviour of composite HTS wires has been reached thanks to the use of two simulation methods, allowing us to develop the distribution of local current density, electrical and magnetic field in the whole range of applied magnetic fields and/or transport currents.

The first method treats the hard superconductor as a conductive medium with highly non-linear current–voltage relation, and allows us to predict nicely the flux penetration. This approach is in agreement with experimental evidence that the relation between the electrical field, E, and the current density can be fairly approximated by the power law relation $E = E_0(\frac{j}{j_0})^n$, where E_0 is the conventional criterion for the determination of the critical current density, j_0, and the exponent n reflects the smoothness of the transition. For an HTS at 77 K, typical values of n are in the range between 15 and 30. This idea was successfully used to predict the influence of the conductor shape on the AC loss [20], to simulate the distribution of currents and AC loss in multifilamentary wires [21] and to calculate the AC loss at in a wire transporting AC current with simultaneous exposure to AC magnetic field [22]. The state equation

$$\nabla \times \frac{1}{\mu_0} \nabla \times \mathbf{A} = \sigma(\mathbf{E}) \cdot \mathbf{E} \tag{3}$$

where

$$\mathbf{E} = -\frac{\partial \mathbf{A}}{\partial t} - \nabla V$$

is to be resolved for the magnetic vector potential $\mathbf{A}$ and the electric potential V. In the case of two-dimensional problems—e.g. for an infinite wire exposed to a perpendicular magnetic field—the cross-section of a superconducting wire is divided into rectangular regions where the conductivity of the superconductor obeys the power law

$$\sigma(E) = \frac{j_0}{E_0}\left(\frac{E}{E_0}\right)^{\frac{1-n}{n}}. \tag{4}$$

An alternative formulation [23] uses the current vector potential $\mathbf{T}$ and magnetic scalar potential Ω. Thorough discussion about the advantages and drawbacks of various formulations for the nonlinear-resistivity approach to the simulation of electromagnetic phenomena in hard superconductors has been published recently [24].

Another numerical simulation method of great practical use is the minimum magnetic energy variation (MMEV) method [25]. Its application is quite straightforward for two-dimensional problems; however, the original formulation [26] is three dimensional [27]. Similarly to the previous method, the cross-section S of the superconductor is divided into rectangular regions; each of them should be filled either with $+j_c$, $-j_c$, or left empty to minimize the functional

$$F[j] = \tfrac{1}{2}\int_S j(\mathbf{r}) A_j(\mathbf{r})\,\mathrm{d}S - \int_S j(\mathbf{r})\widehat{A}_j(\mathbf{r})\,\mathrm{d}S + \int_S j(\mathbf{r})(A_a(\mathbf{r}) - \widehat{A}_a(\mathbf{r}))\,\mathrm{d}S \tag{5}$$

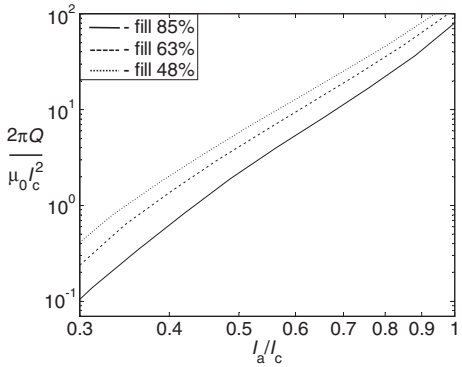

Figure 2. Calculated normalized AC loss, i.e. divided by the loss prefactor proportional to I_c^2, for three cores of superconducting cable differing in the percentage of HTS occupation of the perimeter of the core former. As expected, larger gaps between neighbouring tapes, i.e. lower fill of the core perimeter by HTS tapes, lead to higher AC loss when transporting AC. Kim's dependence of $j_c(B)$ with $j_{c0} = 9.37 \times 10^7$ A m^{-2} and $B_0 = 14$ mT was assumed.

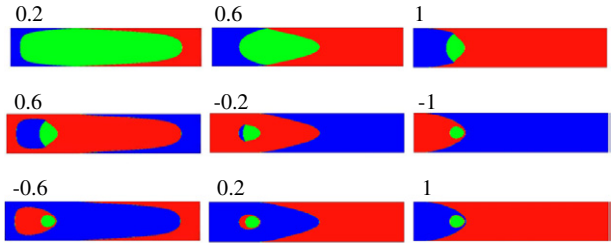

Figure 3. Distribution of current density in the rectangular cross-section of wire made from hard superconductor during simultaneous transport of AC current and application of AC field, calculated with the help of the minimum magnetic energy variation (MMEV) method. AC current amplitude is 60% of the wire critical current, and the magnetic field amplitude is 72% of the penetration field. The sequence of distributions, each characterized by the number indicating the ratio of actual transport current with respect to the amplitude value of AC current, goes from left to right and from top to bottom.

where A_j is the magnetic vector potential created by the currents in the superconductor and A_a is that from the applied field. The quantities with caps correspond to those obtained by the solution in the previous time step. The minimization should obey the constraints

$$I = \int_S j(\mathbf{r})\,\mathrm{d}S$$

$$|j| \leqslant j_c.$$

Thus, the MMEV follows the original idea of the critical state, i.e. the availability of just one value for the current density. In spite of the fact that this is a notable simplification for HTSs, the method offers a distinct shape of the boundaries between positive and negative current density, as well as the shape of the current-free core being precisely found. Then, one can understand the underlying physics of the flux penetration in a given configuration.

3.1. Influence of gaps in transmission cable on its AC loss

Here we show how one can assess the importance of permitting minimum gaps between neighbouring tapes of the single-layer cable as a model arrangement for the power transmission cable. High packing factor—defined as the percentage of the perimeter of the central cylindrical mandrel occupied by the tapes—is not reached easily in the factory production, leading to a significant increase of the manufacturing cost when trying to minimize the gaps. Simulations following Brandt's method [20] allowed us to calculate the quantitative prediction presented in figure 2. We considered 14 tapes placed straight in parallel on the central mandrel of 21 mm diameter. Three cables made from tapes of the same superconducting material but different widths have been compared. The decrease of the tape width leads to a reduction of the cable critical current due to two independent mechanisms: the first is a simple reduction of the superconductor's cross-section, the second is the change of local magnetic field distribution. Therefore, we compare the normalized values of transport AC loss, i.e. divided by the factor proportional to I_c^2. Also, the transport current is normalized with respect to the critical current of the cable in figure 2. In the simulations, the critical current density dependence on local magnetic field was assumed to follow the Kim's relation $j_c(x, y) = \frac{j_{c0}}{1+\frac{|B(x,y)|}{B_0}}$. As one can see, the gaps between tapes can significantly influence the AC loss performance of a power transmission cable.

3.2. AC–AC case for a wire with a rectangular cross-section

The circumstance that commonly a superconducting wire experiences in a cable (made from more wires connected in parallel) or a winding of an electromagnet is that of AC transport under the simultaneous action of the AC field produced by the currents in other wires. The transport current and the magnetic field change in phase. Some basic predictions for these conditions have been derived, but only for the slab geometry [28] or that of an infinitely thin strip [9, 29]. For HTS tapes, the empirical engineering approach based on the fits of experimental data [30] is of practical use; on the other hand, it does not explain why the formulae seem to require modification in some cases. With the help of the MMEV method, it is possible to visualize the movement of flux fronts as the boundaries between zones with different current densities. In figure 3 is shown the evolution of current density distribution in rectangular cross-section of a superconducting conductor with rectangular cross-section (aspect ratio 1:5), calculated with the help of MMEV. Details of the computation can be found elsewhere [31]. The overall picture resembles the results obtained by other methods [22]. Because the boundaries between positive and negative current density, as well as the shape of the current-free core, are clearly determined, one can easily understand why the predictions based on the assumption of a one-dimensional flux penetration—where these boundaries are planar—would not lead to satisfactory agreement with experiment. The predictions of our calculations, performed under assumption of magnetic-field-independent critical current density, have been compared with experimental AC loss data obtained on Bi-2223/Ag multifilamentary tape. In figure 4 is the result

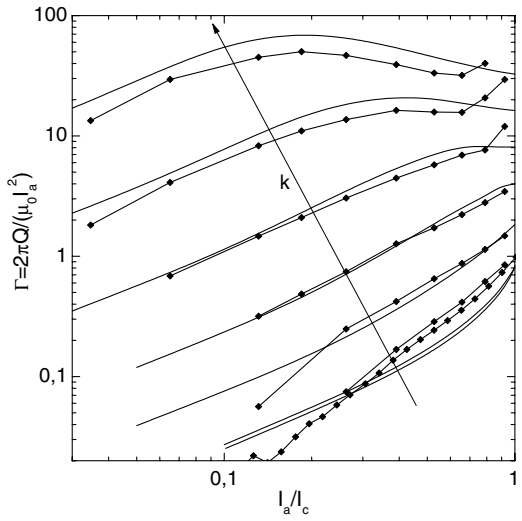

Figure 4. AC loss in Bi-2223 tape transporting AC current with the amplitude I_a under simultaneous action of AC magnetic field with the amplitude B_a. The loss is shown in terms of the loss factor, i.e. the total AC loss divided by the electromagnetic energy, that is proportional to I_a^2, on the AC current amplitude I_a (normalized to I_c) at the condition that B_a increases in proportion to I_a. Theoretical curves (lines) calculated for the proportionality coefficients k in the formula $B_a = \frac{k}{w}\mu_0 I_a$ equal to 0, 0.05, 0.25, 0.5, 0.99, 2, and 4 (from bottom to top) are compared with experimental data plotted by squares.

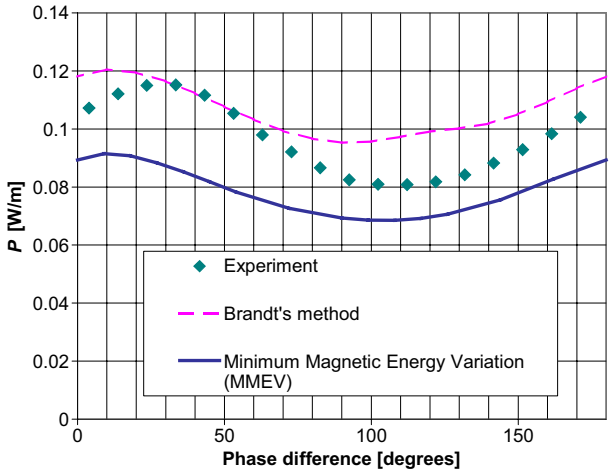

Figure 5. Dependence of AC loss on the phase shift between AC transport current and AC magnetic field of the same frequency. Simulations for a tape 4 mm wide, 0.2 mm thick with the critical current of 38 A, exposed to 10 mT AC field when transporting 17.7 A of AC current, are compared with experimental data. The maximum of dissipation obtained by two different simulation methods as well as that found experimentally is clearly different from the in-phase case.

of this comparison plotted as the normalized loss (sometimes called the loss factor) versus the normalized current, assuming that the applied AC field with the amplitude B_a increases in proportion to the AC current amplitude, I_a. In other words, $B_a = \frac{k}{w}\mu_0 I_a$, where w is the tape width and k is the constant of proportionality. This is the condition representing the most important practical cases, with $k \ll 1$ characterizing the case of prevailing self-field (as in the transmission cable) and $k > 1$ corresponding to the situation met in an electromagnet winding. An interesting feature of the theoretical prediction is that, at low excitations, the loss factor *always* increases with the first power of the current (thus also the first power of the applied field), then in turn predicts a universal loss dependence of a superconducting device at low energizing current as $\propto I_a^3$. Save for the very low k, i.e. the nearly self-field case, the experimental data obey this prediction quite well.

Another interesting situation to investigate in the AC–AC case is the cyclic change of transport current and magnetic field with a certain phase shift between them. This could happen in some important applications like the three-phase transmission line or a transformer winding. We have employed both of the simulation methods mentioned in section 3 to check the AC loss measured on the same Bi-2223/Ag tape. The results are presented in figure 5. A certain deviation between the theoretical predictions based on two different models for superconducting media is not surprising: the loss predicted for the critical-state-like simulation performed by the MMEV method is systematically below the experimental data, while the prediction of the calculation starting from a smooth non-linear $E(j)$ curve with the power exponent $n = 25$ is mostly above them. Interestingly, for all three curves the absolute loss maximum is not found for the in-phase condition. We have found the shift of the loss maximum from zero degrees reproducibly in both the experiments and simulations performed for a wide range of current/field ratios [32].

3.3. *Effect of ferromagnetic cover on AC loss*

Another important problem that can be investigated with the help of the MMEV method is that of a superconductor covered by a ferromagnetic material. Several predictions have been made that such a cover should decrease the AC loss [33, 34], though none of these works has rigorously calculated the flux penetration into hard superconductor put in such a composite structure. Because the MMEV procedure of finding the succession of flux front movements is equivalent to the critical-state approach, the implementation of this method would allow us to perform such a refinement. We have adopted the finite element code FEMLAB to calculate the magnetic field in the simulation box with dimensions ten times exceeding the tape width. The consequence of placing a ferromagnetic strip on a superconducting wire with rectangular cross-section is illustrated in figure 6. The shape of the flux lines and hence the flux penetration front completely changes with respect to a bare superconducting wire. It seems that the ferromagnetic sheath acts as a magnetic mirror, straightening the flux lines inside the superconductor. This would influence the values of penetration field B_p, the diamagnetic susceptibility χ_0 and also the shape of the $\chi''_{int}(y)$ dependence in formula (1). In comparison to the previous work, performed using the ANSYS code with constant permeability of iron [35], we have used the non-linear dependence

$$\mu_r = \frac{\mu_{max}}{1 + \left(\frac{B}{B_c}\right)^2} + 1 \qquad (6)$$

to approximate the non-linear magnetic permeability of the ferromagnetic sheath. At this stage we have not been

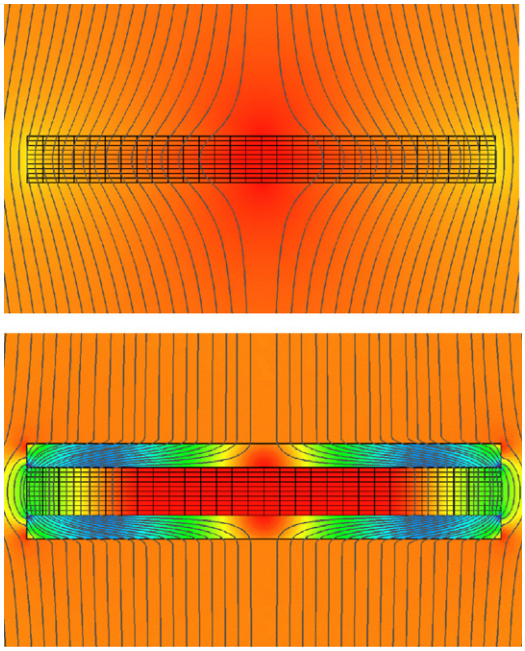

Figure 6. Effect of a ferromagnetic cover on the behaviour of a strip from a hard superconductor exposed to perpendicular magnetic field equal to 50% of the penetration field. A dramatic change of the shape of the flux penetration front as well as a significant reduction of magnetic field inside the superconductor is clearly visible. Non-linear but reversible permeability of the ferromagnetic material was approximated by expression (6) with $\mu_{\max} = 1000$ and $B_c = 0.1$ T.

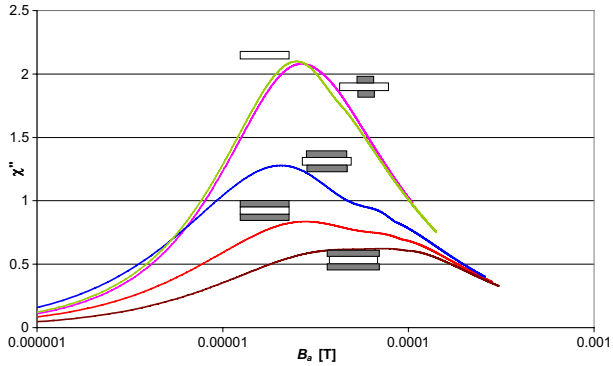

Figure 7. Effect of the completeness of the ferromagnetic sheath cover on the AC loss in an external magnetic field, calculated by the MMEV method. Assuming no hysteresis in the ferromagnetic material, the AC loss—expressed through the imaginary part of AC susceptibility, χ''—is reduced when the ferromagnetic material better covers the superconducting strip.

able to insert the hysteresis of ferromagnetic material in the calculations, and this remains one of the big challenges for this kind of simulations. As an illustration of the predictions we have achieved, we present here the influence of the width of the ferromagnetic cover on the AC susceptibility $\chi'' = \chi_0 \chi''_{\text{int}}$ dependence on the applied magnetic field. One can expect that, depending on how much surface will be covered by a soft magnetic material with necessary thickness, the effect will be more or less visible. This is indeed what we have found, as shown in figure 7. With the narrowing of the ferromagnetic cover, the susceptibility increases approaching that of the bare superconducting wire.

We should underline that, because no hysteresis is considered for the ferromagnetic material, this part of the conductor is not accounted for in the total loss. Such an assumption should be modified when a comparison with experimental data will is carried out. Otherwise, a net reduction of the AC loss results from the covering of the superconductor by a ferromagnetic material.

4. Conclusions

The numerical simulation methods available at the present time to model the electromagnetic behaviour of a hard superconductor represent a significant step forward with respect to the analytical models. Nowadays, two-dimensional problems can be tackled successfully using the Brandt's method or the minimum magnetic energy variation (MMEV) method. This means that the hysteresis loss in single-core wires from hard superconductors of any shape can be predicted at any combination of transport AC current and applied AC magnetic field. In the case of arrays of filaments, the hysteresis loss—i.e. that prevailing at low frequencies—can be calculated as well.

When the coupling current flowing across the metallic matrix in direction perpendicular to the filaments cannot be neglected, the problem becomes three dimensional. For this situation, the approach of representing the hard superconductor as a normal conductor with non-linear current–voltage curve should work as well, as the results achieved with the help of physically justified simplifications have demonstrated [36, 37]. However, the requirements on computing power are still severe and further development for 3D calculations is necessary.

Another field where significant progress is required is the investigation of composites containing superconducting filaments and ferromagnetic parts. Surprisingly, the simulation methods for magnetic hysteresis in superconductors are now better developed than those for ferromagnetic shapes when the exact distribution of local magnetic field is regarded. It would be interesting to see whether a general hysteresis simulation method like the Preisach model [38] could be helpful in resolving this problem.

Acknowledgments

Financial support of this work by the Science and Technology Assistance Agency (contract APVT-20-012902) and the NATO Science programme (grant PST.CLG 980001) is acknowledged.

References

[1] Carr W J Jr 2001 *AC Loss and Macroscopic Theory of Superconductors* 2nd edn (New York: Taylor and Francis)
[2] Hlasnik I 1984 *J. Physique* **45** 459
[3] Wilson M 1983 *Superconducting Magnets* (Oxford: Clarendon)
[4] Kwasnitza K 1977 *Cryogenics* **17** 616
[5] Campbell A M 1982 *Cryogenics* **22** 3
[6] Bean C P 1962 *Phys. Rev. Lett.* **8** 250
London H 1963 *Phys. Lett.* **6** 162

[7] Däumling M and Larbalestier D C 1989 *Phys. Rev.* B **40** 9350
[8] Gömöry F *et al* 2004 *Supercond. Sci. Technol.* **17** S150
[9] Brandt E H and Indenbom M 1993 *Phys. Rev.* B **48** 12893
Brandt E H 1994 *Phys. Rev.* B **49** 9024
[10] Clem J R and Sanchez A 1994 *Phys. Rev.* B **50** 9355
Pardo E, Chen D X, Sanchez A and Navau C 2004 *Supercond. Sci. Technol.* **17** 537
[11] Gömöry F, Hušek I, Kováč P and Kopera L 2000 *Studies of High-Temperature Superconductors* vol 32, ed A Narlikar (New York: Nova Science Publishers) p 63
[12] Gömöry F, Šouc J, Fabbricatore P, Farinon S, Strýček F, Kováč P and Hušek I 2002 *Physica* C **371** 229
[13] Mawatari Y 1996 *Phys. Rev.* B **54** 13215
Mawatari Y 1997 *IEEE Trans. Appl. Supercond.* **7** 1216
[14] Pardo E, Sanchez A and Navau C 2003 *Phys. Rev.* B **67** 104517
[15] Amemiya N, Kasai S, Yoda K, Jiang Z, Levin G A, Barnes P N and Oberly C E 2004 *Supercond. Sci. Technol.* **17** 1464
[16] Norris W T 1970 *J. Phys. D: Appl. Phys.* **3** 489
[17] Inada R, Oota A, Fukunaga T and Fujimoto H 2001 *IEEE Trans. Appl. Supercond.* **11** 2467
[18] Gömöry F and Gherardi L 1997 *Physica* C **280** 151
[19] Fabbricatore P, Farinon S, Innocenti S and Gömöry F 2000 *Phys. Rev.* B **61** 6413
[20] Brandt E H 1996 *Phys. Rev.* B **54** 4246
[21] Amemiya N, Banno N, Inaho K and Tsukamoto O 1995 *IEEE Trans. Magn.* **5** 984
Stavrev S, Grilli F, Dutoit B, Nibbio N, Vinot E, Klutsch I, Meunier G, Tixador P, Yang Y F and Martinez E 2002 *IEEE Trans. Magn.* **38** 849
[22] Zannella S, Montelatici L, Grenci G, Pojer M, Jansak L, Majoros M, Coletta G, Mele R, Tebano R and Zanovello F 2001 *IEEE Trans. Appl. Supercond.* **11** 2441
Tebano R, Mele R, Boffa V, Gomory F, Strycek F and Seiler E 2003 *Int. J. Mod. Phys.* B **17** 528
Amemiya N, Miyamoto K, Murasawa S, Mukai H and Ohmatsu K 1998 *Physica* C **310** 30
Amemiya N and Ohta Y 2001 *Physica* C **357–360** 1134
Stavrev S, Grilli F, Dutoit B and Ashworth S P 2005 *Supercond. Sci. Technol.* **18** 1300
[23] Amemiya N, Murasawa S, Banno N and Miyamoto K 1998 *Physica* C **310** 16
[24] Grilli F, Stavrev S, Le Floch Y, Costa-Bouzo M, Vinot E, Klutsch L, Meunier G, Tixador P and Dutoit B 2005 *IEEE Trans. Appl. Supercond.* **15** 17
[25] Sanchez A and Navau C 2001 *Phys. Rev.* B **64** 214506
Sanchez A and Navau C 2001 *Supercond. Sci. Technol.* **14** 444
Pardo E, Sanchez A, Chen D X and Navau C 2005 *Phys. Rev.* B **71** 134517
[26] Prigozhin L 1996 *J. Comput. Phys.* **129** 190
Prigozhin L 1997 *IEEE Trans. Appl. Supercond.* **7** 3866
[27] Bhagwat K V, Nair S V and Chaddah P 1994 *Physica* C **227** 176
Badia A and Lopez C 2001 *Phys. Rev. Lett.* **87** 127004
Badia A and Lopez C 2002 *Phys. Rev.* B **65** 104514
[28] Carr W J Jr 1979 *IEEE Trans. Magn.* **15** 240
[29] Zeldov E, Clem J R, McElfresh M and Darwin M 1994 *Phys. Rev.* B **49** 9802
[30] Rabbers J J, ten Haken B and ten Kate H H J 2003 *IEEE Trans. Appl. Supercond.* **13** 1731
[31] Pardo E, Gömöry F, Chen D X, Sanchez A and Navau C 2005 *EUCAS 2005 Conf.* (poster TH-P4-57)
[32] Vojenčiak M, Šouc J, Ceballos J, Klinčok B, Gömöry F, Pardo E and Grilli F 2005 *EUCAS 2005 Conf.* (poster MO-P1-34)
[33] Majoros M, Glowacki B A and Campbell A M 2000 *Physica* C **334** 129
Majoros M, Glowacki B A and Campbell A M 2001 *IEEE Trans. Appl. Supercond.* **11** 2780
Glowacki B A, Majoros M, Rutter N A and Campbell A M 2001 *Cryogenics* **41** 103
[34] Genenko Y A 2002 *Phys. Status Solidi* a **189** 469
Yampolskii S V and Genenko Y A 2005 *Phys. Rev.* B **71** 134519
[35] Farinon S, Fabbricatore P, Gömöry F, Greco M and Seiler E 2005 *IEEE Trans. Appl. Supercond.* **15** 2867
[36] Amemiya N, Jin F, Jiang Z, Shirai S, ten Haken B, Rabbers J J, Ayai N and Hayashi K 2003 *Supercond. Sci. Technol.* **16** 314
[37] Bouzo M C, Grilli F and Yang Y 2004 *Supercond. Sci. Technol.* **17** 1103
[38] Sjostrom M 2004 *Physica* B **343** 96